Analysis of local ventricular repolarization using unipolar recordings in patients with arrhythmogenic right ventricular cardiomyopathy

Maciej Kubala[1,2] · Shuanglun Xie[1] · Pasquale Santangeli[1] · Fermin C. Garcia[1] · Gregory E. Supple[1] · Robert D. Schaller[1] · Jackson J. Liang[1] · Rajeev K. Pathak[1] · Erica S. Zado[1] · Cory Tschabrunn[1] · Jeffrey Arkles[1] · David J. Callans[1] · Francis E. Marchlinski[1]

Abstract

Purpose In arrhythmogenic right ventricular cardiomyopathy (ARVC), abnormal electroanatomic mapping (EAM) areas are proportional to extent of T-wave inversion on 12-lead ECG. We aimed to evaluate local repolarization changes and their relationship to EAM substrate in ARVC.

Methods Using unipolar recordings, we analyzed the proportion of negative T waves ≥ 1 mV in depth (NegT), NegT area, Q-Tpeak (QTP), Tpeak-Tend (TPE) intervals and their relationship to bipolar (< 1.5 mV ENDO, < 1.0 mV EPI) and unipolar (< 5.5 mV) endocardial (ENDO) and epicardial (EPI) low-voltage area (LVA) in 21 pts. (15 men, mean age 39 ± 14) with ARVC. Control group included 5 pts. with normal hearts and idiopathic PVCs.

Results On ENDO, the % of NegT ($7 \pm 5\%$ vs $30 \pm 20\%$, $p = 0.004$) and the NegT area (12.9 ± 9.7 c m^2 vs 61.4 ± 30.0 cm^2, $p = 0.001$) were smaller in ARVC compared to controls. On EPI, the % of NegT was similar ($5 \pm 7\%$ vs $3 \pm 4\%$, $p = 0.323$) and the NegT area, larger (11.0 ± 8.4 cm^2 vs 2.7 ± 0.9 cm^2, $p = 0.027$) in ARVC group. In ARVC group, the % of NegT area inside LVA was larger on EPI compared to ENDO for both bipolar ($81 \pm 27\%$ vs $31 \pm 33\%$, $p < 0.001$) and unipolar ($90 \pm 19\%$ vs $73 \pm 28\%$, $p = 0.036$) recordings. Compared to normal voltage regions, QTP inside ENDO abnormal LVA was on average 58 ± 26 ms shorter and TPE, 25 ± 56 ms longer (97 ± 26 ms and 56 ± 86 ms on EPI, respectively).

Conclusions In ARVC, NegT areas are more closely associated with abnormal depolarization LVA on the EPI and QTP is shorter and TPE longer inside ENDO and EPI abnormal LVA compared to normal voltage regions. The results add to our understanding of ARVC arrhythmia substrate.

1 Introduction

Arrhythmogenic right ventricular cardiomyopathy (ARVC) is a myocardial disease characterized by fibrofatty replacement of ventricular myocytes resulting in ventricular arrhythmias [1]. Frequent intramural and epicardial (EPI) involvement and the presence of patchy or layered scar in ARVC complicate the detection and precise location of the underlying substrate. The Revised Task Force diagnostic criteria for ARVC include depolarization and repolarization abnormalities on the surface ECG [2]. Correlation between depolarization and repolarization abnormalities with abnormal electroanatomical voltage have been previously demonstrated [3, 4]. A number of approaches for substrate-based mapping and ablation in sinus or paced rhythm have been described [5]. Importantly, methods targeting arrhythmogenic regions defined as zones of slow conduction based on identification of abnormal electrograms within low-voltage areas are all limited by the imprecise definition of the substrate [5]. Little is known about the genesis of negative T waves (NegT) in ARVC and their correlation with arrhythmogenic substrate or disease severity.

✉ Francis E. Marchlinski
francis.marchlinski@uphs.upenn.edu

[1] Cardiac Electrophysiology Program, Cardiovascular Division Hospital of the University of Pennsylvania, 9 Founders Pavilion – Cardiology, 3400 Spruce St., Philadelphia, PA 19104, USA

[2] Cardiac Arrhythmia Unit, Amiens-Picardie University Hospital, Amiens, France

Increased action potential gradients between EPI and endocardium (ENDO) are required for T-wave inversion [6, 7].Changes in local action potential duration due to progression of an underlying pathologic process can result in intrinsic electrical heterogeneity and reversed repolarization sequence [8, 9]. We have recently demonstrated the relationship of the RV EAM ENDO and EPI abnormal areas to the extent and location of T-wave inversion on 12-lead ECG [10]. Unipolar ENDO and EPI electrograms have been previously used to study repolarization abnormalities in animal models [11–13]. Preliminary studies in humans reported increased repolarization heterogeneity observed in unipolar ENDO and EPI recordings in patients with cardiomyopathy and history of ventricular arrhythmia [9, 14–16]. Recently, repolarization changes observed in unipolar recordings have been used to identify functional substrate and to evaluate acute results of radiofrequency ablation in Brugada syndrome [17].

Using unipolar recordings, we aimed to describe ENDO and EPI distribution and characteristics of NegT and their relationship to bipolar and unipolar depolarization voltage abnormalities in the setting of ARVC patients to gain additional insight into the arrhythmogenic substrate.

2 Methods

2.1 Study population

We included 21 patients referred for VT ablation at the Hospital of the University of Pennsylvania who underwent detailed electroanatomic voltage mapping (EAM). All patients met the revised 2010 Task Force Criteria (2 major criteria or 1 major criterion plus 2 minor criteria or 4 minor criteria) for the diagnosis of definite ARVC [2]. All ablation procedures were performed following institutional guidelines. Amiodarone was discontinued for at least 1 month and other antiarrhythmic medication for at least five half-lives prior to ablation unless being used to treat frequent recurrent VT or VT storm. Patients who were pacemaker-dependent and had no underlying rhythm were excluded. All patients provided written informed consent for electrophysiological study and participation in data collection and reporting. A control group consisted of 5 patients with normal hearts (normal transthoracic echocardiogram and/or cardiac magnetic resonance imaging (MRI) with no low-voltage abnormalities on EAM), referred for ablation of idiopathic premature ventricular contractions (PVCs). All controls underwent ENDO and EPI detailed EAM.

2.2 Electroanatomic endocardial voltage mapping

Patients underwent detailed EAM using The CARTO EAM system (Version XP and 3, Biosense Webster, Diamond Bar, CA) as previously described [18–20]. The studies were performed under conscious sedation or general anesthesia. An intracardiac echo catheter (Acuson Acunav; Siemens, Mountain View, CA) was systematically used and advanced into the right atrium or the RV to define RV anatomy, guide anatomic positioning and confirm contact of the mapping catheter. For each patient, an EAM of the RV endocardium was created using a standard 3.5 mm tip, 2 mm ring open-irrigated catheter with 2–5–2 mm spacing for sensing electrodes (Navistar Thermocool; Biosense Webster) and maintaining a fill threshold of < 15 mm. Bipolar electrograms were filtered at 30 to 500 Hz, displayed at 200 mm/s sweep speed, and stored for offline annotation and analysis. Unipolar electrograms were recorded (bandpass filtered at 1–240 Hz) and stored simultaneously. An EAM area was considered abnormal at sites where multiple contiguous low-voltage bipolar (< 1.5 mV signal amplitude) or unipolar (< 5.5 mV) electrograms were present.

2.3 Electroanatomic epicardial voltage mapping

Epicardial access to the pericardial space was obtained using a Tuohy needle as described by Sosa et al. [21]. A posterior approach was typically used when approaching the pericardium because of the RV dilation frequently encountered. All aspects of the RV EPI were sampled using a standard 3.5-mm tip, 2-mm ring open-irrigated catheter maintaining a fill threshold of < 20 mm. To limit the influence of EPI fat and coronary vasculature, a lower voltage cutoff < 1.0 mV was utilized to define EPI voltage abnormalities [18, 22]. Furthermore, to help distinguish low amplitude EPI electrograms due to fat, epicardial bipolar electrograms were defined as abnormal if (1) wide: 80 ms duration; (2) split: 2 or more distinct components with 20 ms isoelectric segment between peaks of individual components or (3) late: distinct electrograms with onset after the end of the QRS complex [22, 23]. In order to minimize the heterogeneity of sampling across the study cohort, the proportion of abnormal bipolar electrograms was calculated by reporting the ratio of the number of abnormal electrograms over the total point acquisition count in each patient. To align abnormal EPI substrate opposite to the ENDO anatomic shell, we used a 0.5- to 1.0-cm margin from the anatomically defined large coronary vessels (right coronary artery or left anterior descending coronary artery) anatomy with the use of coronary angiography, merged computed tomographic images, or both.

2.4 Analysis of the negative T waves in unipolar recordings

Unipolar electrograms of all sampled ENDO and EPI points were visualized in the selected point viewer (Carto system) during offline analysis. Analysis of the T-wave morphology was performed in sinus rhythm at the 100 mm/s speed using

unipolar tracings recorded from the distal electrode of the mapping catheter. A NegT was defined as downward directed, entirely below the isoelectric level (which was defined by TP segment) T wave ≥ 1 mV in depth. Biphasic T waves were considered as having 2 opposed directional components. Complexes following PVCs, runs of VT and paced ventriculograms were excluded from the analysis in order to avoid evaluation errors resulting from cardiac memory. The ENDO and EPI areas of NegT were evaluated using the Carto system area measurement tool. The points at the limit of the NegT area were used as vertices of a figure to assess the surface. If the distance between NegT points was less than 3 cm, then the points were considered as belonging to the same area.

Points at distance more than 3 cm were considered as belonging to different areas which were eventually added together. Proportion of NegT to total number of points sampled, NegT EAM area, and the relationship of NegT areas with bipolar and unipolar low-voltage regions for ENDO and EPI were compared with the control group. Locations of entrainment with concealed fusion or optimal pace matches and VT termination during ablation, when available, were compared with locations with NegT.

The Q-Tpeak and Tpeak-Tend intervals were obtained from unipolar recordings in which the NegT were observed. The earliest onset of the QRS of each electrogram was used as a starting point. The peak of the NegT was defined as the time point of maximum T-wave amplitude. The end of the T wave was defined as the point of intersection of a line tangential to the point of a maximal slope with isoelectric level. The mean value of 3 measurements of different NegT points (mean value of 3 complexes for each point) of the same area was reported for bipolar low and normal voltage areas. Q-Tpeak, and Tpeak-Tend intervals of NegT points were compared between bipolar low and normal voltage areas.

2.5 Definition of right ventricular segments

Using a modified version of a previously reported RV free wall scoring model, RV was divided into distinct anatomic segments as follows (Fig. 1): from the pulmonary valve to the top of the tricuspid valve—RV outflow tract (RVOT) region, top of the tricuspid valve to mid tricuspid valve (mid-RV body), and mid tricuspid valve to bottom of the RV (inferior RV body) [24]. The mid-RV and inferior RV body was further divided into three regions: a basal region extending from the tricuspid valve to 2 cm anterior of the valve, and two equal portions between this region and the RV apex (free wall and apical region). This resulted in 7 anatomic segments shown on Fig. 1. A segment was considered abnormal if reproducible signal abnormalities (low or very low voltage associated with abnormal bipolar electrograms as previously described) were identified within and > 5 mm away from the pulmonic or tricuspid valve annuli. To
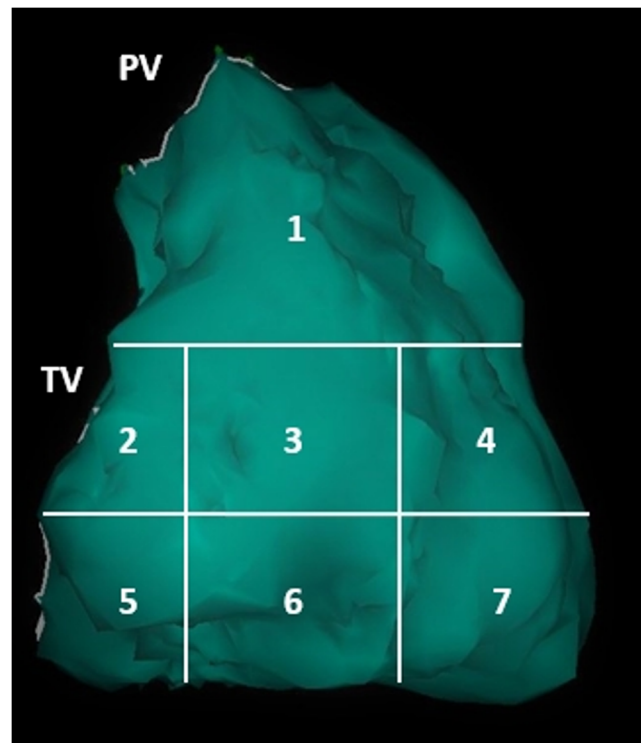

Fig. 1 Schematic right anterior oblique view of the right ventricle divided into segments. Schematic right anterior oblique view of the right ventricular free wall divided into 7 segments. To facilitate the analysis, segments 2 and 3 were merged forming RV mid-free wall region, 5 and 6—inferior region, 4 and 7—apical region for the analysis. *PV* pulmonary valve, *TV* tricuspid valve

facilitate the analysis, segments 2 and 3 were merged to form RV mid-free wall region, 5 and 6 to form inferior region and segments 4 and 7 to form apical region.

2.6 Statistical analysis

Discrete variables were reported as percentages and continuous variables as mean and standard deviations. The differences between groups were tested with Fisher's exact test for discrete variables and with Student's t test or Mann-Whitney U test as appropriate test for continuous variables. A two-sided $p < 0.05$ was considered statistically significant. Statistical analysis was performed using the SPSS software package, version 22 (SPSS Inc.).

3 Results

The study population included 21 patients (15 [71%] men) with a mean age of 39.4 ± 14.5 years. Patients' characteristics are shown in Table 1. All patients fulfilled revised Task Force criteria for ARVC and met an average 1.9 ± 1.2 major criteria and 0.9 ± 1.0 minor criteria. Structural abnormalities were documented by cardiac MRI performed in 15 (71%) patients. All patients had

Table 1 Baseline characteristics

Characteristic	$n = 21$
Age of ARVC diagnosis, year	39.4 ± 14.5
Sex, male	12 (57%)
History of cardiac arrest or syncope	9 (42%)
Implantable cardioverter defibrillator	16 (76%)
LV ejection fraction, %	57 ± 3
Task force criteria—major	
Structural	10 (47%)
Depolarization	7 (33%)
Repolarization	8 (38%)
Arrhythmias	13 (61%)
Family history	2 (9%)
Average per patient	1.9 ± 1.2
Task force criteria—minor	
Structural	4 (19%)
Depolarization	3 (14%)
Repolarization	6 (28%)
Arrhythmias	9 (42%)
Family history	1 (4%)
Average per patient	0.9 ± 1.0

documented recurrent symptomatic VT. A control group included 5 patients (3 [60%] men, mean age 49 ± 5 years) who underwent a radiofrequency ablation of idiopathic PVCs.

3.1 Electroanatomic mapping

In the ARVC group, the ENDO low-voltage area was greater for unipolar compared to bipolar recordings ($47.0 \pm 23.5\%$ vs $16.0 \pm 13.7\%$, $p < 0.001$). Abnormal low bipolar voltage areas were less extensive on the ENDO vs the EPI ($16.0 \pm 13.7\%$ vs $44.8 \pm 24.6\%$, $p < 0.001$). Mean number of RV segments with abnormal bipolar voltage and abnormal electrograms was lower on ENDO vs EPI (2.2 ± 1.4 vs 4.1 ± 2.1, $p < 0.001$). ENDO low-voltage abnormalities were present in RVOT or RV mid-free wall region in 17 (81%) patients, in inferior region in 13 (62%) and in apical region in 2 (9%) patients. Low-voltage EPI abnormalities were observed in 20 (95%) patients in RVOT or RV mid-free wall region, in 17 (81%) in inferior region and in 7 (33%) patients in apical region. The comparison of electroanatomical findings between ARVC patients and the control group is shown in Table 2.

3.2 Negative T waves in unipolar recordings and voltage abnormalities

On the ENDO, the proportion of NegT ($7 \pm 5\%$ vs $30 \pm 20\%$, $p = 0.004$) and the NegT EAM area (12.9 ± 9.7 cm^2

vs 61.4 ± 30.0 cm^2, $p = 0.001$) were smaller as compared with the control group. In the ARVC group, $31 \pm 33\%$ of NegT area was inside the low-voltage ENDO bipolar area (Fig. 2) and $73 \pm 28\%$ inside the low-voltage unipolar area. In the control group, NegT were observed in 5 (100%) patients in 3 regions described above (Fig. 3).

On the EPI, the proportion of NegT was similar ($5 \pm 7\%$ vs $3 \pm 4\%$, $p = 0.323$) while the NegT EAM area larger in ARVC group than in the control group (11.0 ± 8.4 cm^2 vs 2.7 ± 0.9 cm^2, $p = 0.027$). Overall, $81 \pm 27\%$ of NegT area was inside the low-voltage EPI bipolar area (Fig. 4) and $90 \pm 19\%$ inside the low-voltage unipolar area. In the control group, NegT were observed in 3 (60%) patients in RVOT or RV mid-free wall region and no NegT were present in inferior and apical segments. The proportion of NegT area inside the low-voltage area was larger on the EPI compared to ENDO for both bipolar ($81 \pm 27\%$ vs $31 \pm 33\%$, $p < 0.001$) and unipolar ($90 \pm 19\%$ vs $73 \pm 28\%$, p 0.036) recordings. The relationships of distribution and characteristics of negative T waves observed with unipolar recordings, and bipolar ENDO and EPI depolarization voltage abnormalities in ARVC patients are shown in Table 3. Fourteen (66%) documented locations of entrainment data consistent with clinical VT or VT termination during ablation coincided with the identified areas of NegT.

3.3 Q-T peak and T peak-T end intervals and voltage abnormalities

Q-T peak and T peak-T end intervals corresponding to all points with NegT were similar in ARVC patients compared to the control group (Table 2). In ARVC patients, Q-T peak intervals were on average 58 ± 26 ms shorter and Tpeak-Tend intervals were 25 ± 56 ms longer inside ENDO low-voltage area compared to normal voltage regions. On the EPI, Q-T peak intervals were on average 97 ± 46 ms shorter while Tpeak-Tend intervals were 56 ± 86 ms longer. Differences in Q-Tpeak and Tpeak-Tend intervals between normal voltage area and regions with low-voltage abnormalities are shown in Table 3 and illustrated in Figs. 2 and 3. Figure 5 shows a repolarization map created for the same patients based on T-wave peak (negative, biphasic or positive T waves) of all sampled points (R wave in lead V6 was used as reference). Change of T peak timing generated a visible color change at the location corresponding to the edge of standardly defined abnormal depolarization low voltage regions. In the control group, QT peak interval was homogenous on the ENDO and EPI surface (Fig. 6). A difference of 17 ± 5 ms between Q-Tpeak interval (NegT) at the apex and the same interval at the base was observed.

4 Discussion

4.1 Main findings

The results of this study add to the fundamental knowledge of the underlying substrate in ARVC. We describe the distribution and relationship of negative T waves observed in unipolar recordings with low voltage depolarization abnormalities in ARVC. The main findings of this study are as follows:

1). On the ENDO, the number and distribution of NegT using unipolar recordings is more limited in ARVC patients compared to controls. On the EPI, the NegT area is larger in ARVC patients.
2). The NegT areas are more closely associated with standardly defined abnormal depolarization low-voltage regions on the EPI. Clinical VT entrainment data and ablation sites also coincide with NegT area.
3). Q-Tpeak intervals corresponding at sites of NegT waves are shorter and Tpeak-Tend intervals longer inside ENDO and EPI abnormal low voltage areas compared to normal voltage regions.

The concordance of the QRS and T waves is dependent on the relationship between epicardial activation and repolarization times [25, 26]. Both activation and recovery occur as propagated waveforms. Sites that are activated late have shorter repolarization times [9, 27]. Accordingly, sites involved in a pathological process resulting in later activation may repolarize earlier resulting in discordance of QRS and T waves. In humans, the changes of the direction of the T waves are also conditioned by apico-basal differences in repolarization time [11, 28]. Moreover, the loss in inverse relation between the action potential duration and the activation time results in the T-wave inversion [29]. We have recently demonstrated that the EAM abnormal endocardial and epicardial bipolar and endocardial unipolar voltage areas were proportional to the extent of T-wave inversion on 12-lead ECG in ARVC [10]. Region-specific surface ECG T-wave abnormalities correlated with corresponding endocardial and epicardial electroanatomic substrates. The actual study adds a new information on the relationship of repolarization abnormalities to electroanatomic substrate. Using local unipolar recordings, we show that the NegT areas observed on the epicardium more frequently than in the control group and associated with abnormal depolarization low voltage areas, appear to be a marker of a pathological process. The question whether the presence of NegT in normal voltage area can be interpreted as an early pathological involvement remains unanswered. However, a lower peak to peak voltage of NegT inside normal voltage areas compared to the controls might suggest the presence of different electrical characteristics in a specific region.

Table 2 Comparison of EAM findings and characteristics of negative T waves observed in unipolar recordings between ARVC patients and the control group

Variable	ARVC $n = 21$	Control group $n = 5$	p
ENDO			
Total endocardial surface (cm^2)	207.9 ± 60.8	206.8 ± 40.3	0.922
Number of points sampled	316 ± 106	218 ± 106	0.079
Abnormal electrograms, %	12.0 ± 5.0	0.2 ± 0.4	0.001
Points with negative T waves, %	7 ± 5	30 ± 20	0.004
NegT EAM area, cm^2	12.9 ± 9.7	61.4 ± 30.0	0.001
NegT points amplitude peak to peak inside > 1.5 mV bipolar area, mV	5.0 ± 1.9	7.3 ± 1.2	0.030
NegT QRS onset-Tpeak, ms	351 ± 38	357 ± 22	0.907
NegT Tpeak-Tend, ms	149 ± 53	179 ± 59	0.228
EPI			
Total epicardial surface (cm^2)	175.2 ± 58.9	212.7 ± 119.2	0.335
Number of points sampled	326 ± 169	196 ± 152	0.165
Abnormal electrograms, %	18 ± 7	1 ± 1	< 0.001
Points with negative T waves, %	5 ± 7	3 ± 4	0.323
NegT EAM area, cm^2	11.0 ± 8.4	2.7 ± 0.9	0.027
NegT points amplitude peak to peak inside > 1.0 mV bipolar area, mV	5.6 ± 2.3	6.8 ± 0.1	0.196
NegT points QRS onset-Tpeak, ms	405 ± 63	430 ± 42	0.637
NegT points Tpeak-Tend, ms	149 ± 65	145 ± 21	0.228

EAM electroanatomic voltage mapping, *ENDO* endocardium, *EPI* epicardium, *NegT* negative T wave

Fig. 2 Representative example of ENDO bipolar low voltage (< 1.5 mV) abnormalities in antero-posterior view in patient with ARVC. Orange dots represent points with NegT in unipolar recordings. Other sampled points manifest positive or biphasic T waves. Thirty-five percent of NegT EAM area is inside abnormal low voltage area. Blue dot corresponds to the site of VT termination. Q-T peak interval is shorter and T peak-T end interval longer inside the abnormal low-voltage area compared to normal voltage region. *EAM* electroanatomic map
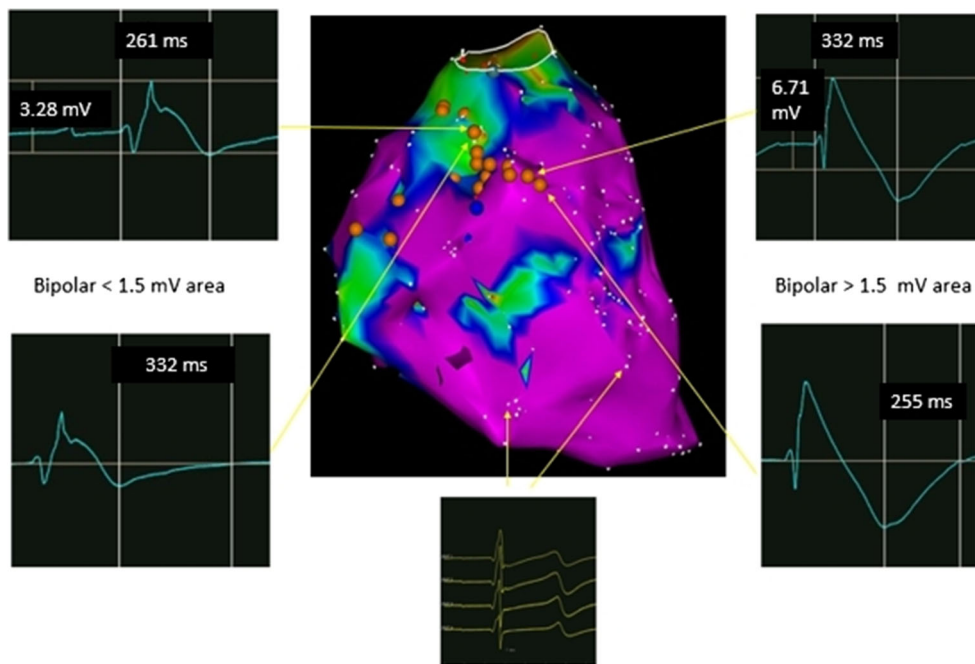
On the ENDO, the proportion of NegT was greater in the control group compared with ARVC patients. Body surface ECG reflects voltage distribution on the epicardium [11, 28]. In the normal heart, there is inversion of the repolarization vector along opposite sides of the myocardial wall: anterior RV electrograms typically have positive T waves, whereas those recorded posteriorly typically manifest negative T waves. For that reason, interpretation of the polarity of ENDO T waves in ARVC patients in this context is difficult. Further analysis of positive or biphasic T waves could be of interest.

This study also demonstrates the presence of Q-Tpeak interval shortening within both ENDO and EPI areas with low voltage abnormalities. This observation is in line with observations showing that repolarization becomes more rapid when activation time lengthens, as previously reported [27]. Interestingly, NegT observed in limited areas within or at the limit of low-voltage regions were situated inside the zones targeted with radiofrequency ablation. The target areas were defined using the conventional criteria based on entrainment or analysis of the abnormal depolarization signals used to identify the arrhythmogenic substrate. Shortening of the Q-Tpeak interval suggest that areas of slow conduction can be identified by analyzing repolarization patterns. Moreover, the described repolarization changes seem to be limited to restricted areas which could represent a potential target for more limited ablation. However, these findings were obtained in patients at different stages of the pathological process and further studies are needed in larger populations to define more precisely the arrhythmogenic substrate associated with local repolarization abnormalities.

Longer Tpeak-Tend interval corresponding to local dispersion of repolarization has been reported as a marker of

Fig. 3 **a** Endocardial (< 1.5 mV) and **b** epicardial (< 1.0 mV) electroanatomic voltage maps from one of the patients without structural disease (control group). Orange dots represent points with NegT in unipolar recordings. ENDO NegT EAM area = 30 cm^2 (26% of the total RV surface). EPI NegT area = 3 cm^2 (5% of the total RV surface)
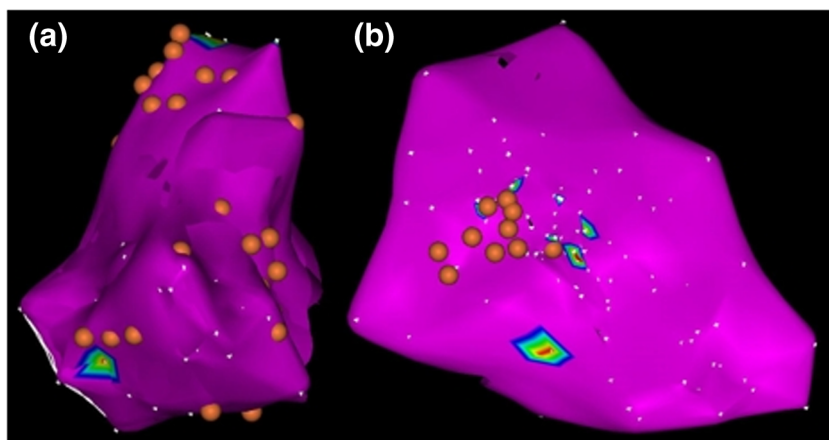
Fig. 4 Representative example of EPI bipolar low voltage (< 1.0 mV) abnormalities in antero-posterior view in patient with ARVC. Orange dots represent points with NegT in unipolar recordings. Black dots represent late potentials. Seventy-nine percent of EAM NegT area is inside abnormal low-voltage area. Q-T peak interval is shorter and T peak-T end interval longer inside the abnormal low voltage area compared to normal voltage region
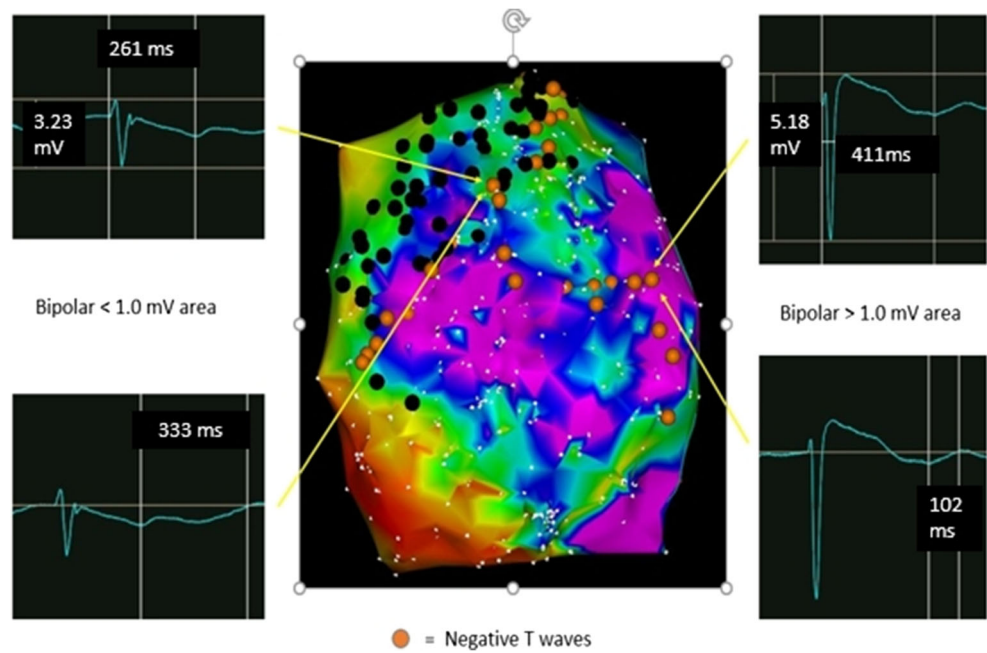
arrhythmogenicity [30, 31]. Prolonged Tpeak-Tend interval in low voltage areas was observed in our study. However, the interpretation of the Tpeak-Tend interval can be limited by difficulties in defining the precise the end of the T wave [32]. In perfused canine wedge preparations, prior research has shown that the peak of the T wave coincided with the end of the EPI repolarization [8, 33]. However, these findings have not been confirmed in human hearts.

Given the important role of repolarization abnormalities in arrhythmogenesis, the ability to further delineate substrate with abnormal repolarization is of clinical significance.

Repolarization data provided in this study illustrates a complex architecture of the scar which is more complicated than that defined by analysis of voltage depolarization abnormalities alone. T-wave morphology and Q-Tpeak intervals can be easily visualized and interpreted during the procedure. Repolarization mapping could thus be considered as a helpful adjunctive strategy for functional identification of the arrhythmogenic substrate providing additional information to activation only based methods. Our findings and the potential usefulness of analyzing T waves to identify ablation targets need to be confirmed with further studies. Specifically, prospective studies using pacing maneuvers

Table 3 Relationship of distribution and characteristics of negative T waves observed in unipolar recordings with bipolar ENDO and EPI depolarization voltage abnormalities in ARVC patients

Variable			p value
ENDO	Bipolar < 1.5 mV area	Bipolar > 1.5 mV area	
	$n = 21$	$n = 21$	
NegT EAM surface (cm^2)	3.7 ± 6.0	9.3 ± 8.1	0.033
NegT points amplitude peak to peak, mV	1.9 ± 0.7	5.2 ± 1.9	< 0.001
NegT points QRS onset-Tpeak, ms	290 ± 40	351 ± 41	0.001
NegT Tpeak-Tend, ms	167 ± 74	148 ± 47	0.066
EPI	Bipolar < 1.0 mV area	Bipolar > 1.0 mV area	
NegT EAM surface (cm^2)	8.0 ± 7.1	2.8 ± 5.2	0.023
NegT points amplitude peak to peak, mV	2.0 ± 0.5	5.6 ± 2.3	0.001
NegT points QRS onset-Tpeak, ms	312 ± 40	405 ± 62	0.001
NegT points Tpeak-Tend, ms	210 ± 81	154 ± 67	0.001

EAM electroanatomic voltage mapping, *ENDO* endocardium, *EPI* epicardium, *NegT* negative T wave

Fig. 5 Representative examples of **a** ENDO bipolar low voltage (< 1.5 mV) abnormalities in antero-posterior view, **b** ENDO repolarization map based on Q-T peak of all sampled points of the same patient with ARVC, **c** EPI epicardial bipolar low voltage (< 1.0 mV) abnormalities, and **d** epicardial repolarization map based on Q-T peak of all sampled points from the same patient with ARVC as in C. Black dots represent sites with late potentials. Orange dots represent points with NegT on unipolar recordings. Yellow asterisk represents the spot of the VT termination. **b** ENDO repolarization map. Color scale was adjusted between 220 and 280 ms. Purple color corresponds to area with Q-Tpeak intervals > 280 ms and green and red to progressively shortened Q-T peak intervals
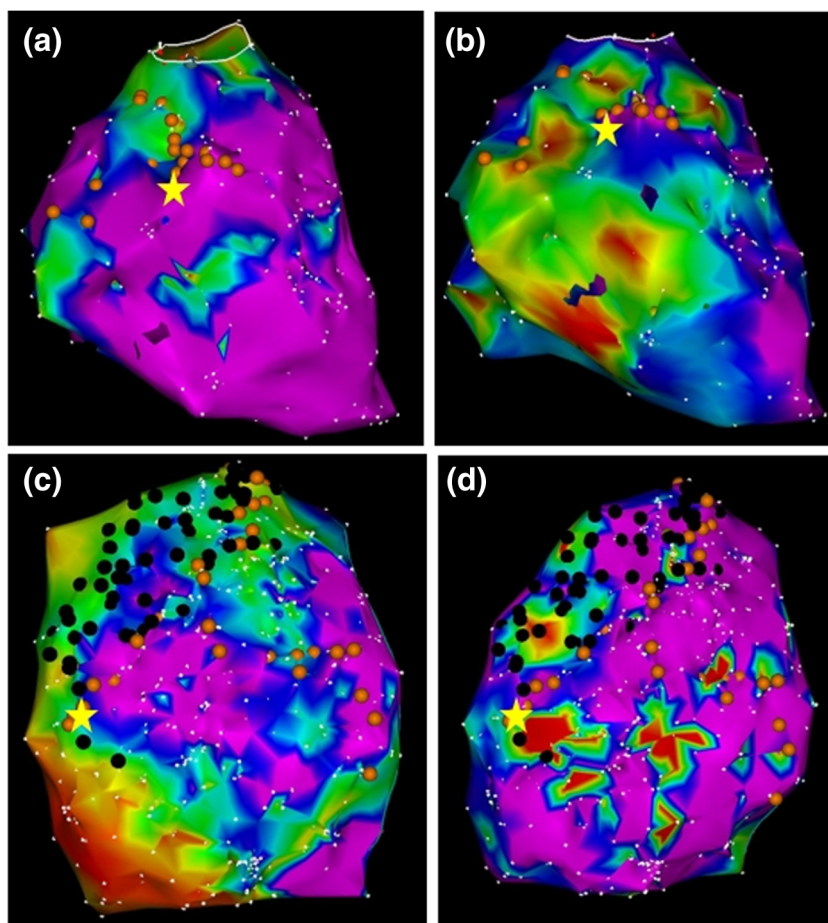
would also be of interest to describe more precisely the areas with NegT and their relationship with the regions critical for maintenance of VT. Identification of these critical sites could allow for more refined, less extensive substrate ablation while still achieving adequate long-term arrhythmia elimination.
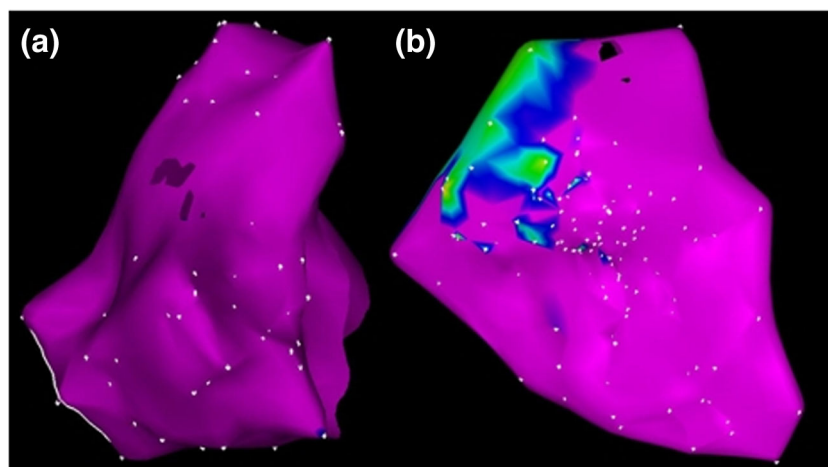

Fig. 6 **a** Endocardial and **b** epicardial repolarization maps from patient without structural disease (control group) based on Q-T peak of all sampled points. Orange dots represent points with NegT in unipolar recordings. Yellow asterisk represents the spot of the VT termination. Color scale was adjusted between 220 and 260 ms for ENDO and 220–280 ms for EPI. Purple color corresponds to area with Q-Tpeak intervals > 260 ms (ENDO) and > 280 ms (EPI). Of note, on the ENDO, the repolarization map is a uniform purple color corresponding with homogenous Q-T peak intervals. On the EPI, the mean difference between apical and basal Q-T peak intervals reached 17 ± 5 ms

4.2 Limitations

This is a retrospective study in a select group of patients with ARVC with more extensive epicardial substrate and it is possible that results may not apply to other disease states. Insufficient density of collected points could result in non-identification of NegT areas; however, care was taken to perform detailed mapping. Finally, frequent changes in activation pattern during ablation procedures could impact repolarization but care was taken to record during steady state sinus rhythm to avoid this confounder.

5 Conclusions

Repolarization analysis using unipolar recordings during sinus rhythm enables visualization of NegT areas associated with epicardial depolarization low voltage areas. Shortening of Q-Tpeak intervals is observed inside both ENDO and EPI areas with standardly defined low voltage abnormalities. Analysis of repolarization heterogeneity in ARVC may be a helpful tool to identify and further characterize the arrhythmogenic substrate targeted during VT ablation in patients with ARVC.

References

1. Basso C, Corrado D, Marcus FI, Nava A, Thiene G. Arrhythmogenic right ventricular cardiomyopathy. Lancet. 2009;373(9671):1289–300.

2. Marcus FI, McKenna WJ, Sherrill D, Basso C, Bauce B, Bluemke DA, et al. Diagnosis of arrhythmogenic right ventricular cardiomyopathy/dysplasia: proposed modification of the task force criteria. Circulation. 2010;121(13):1533–41.

3. Tanawuttiwat T, et al. Electroanatomic correlates of depolarization abnormalities in arrhythmogenic right ventricular dysplasia/cardiomyopathy. J Cardiovasc Electrophysiol. 2016;27(4):443–52.

4. Zorzi A, et al. Electrocardiographic predictors of electroanatomic scar size in arrhythmogenic right ventricular cardiomyopathy: implications for arrhythmic risk stratification. J Cardiovasc Electrophysiol. 2013;24(12):1321–7.

5. Santangeli P, Marchlinski FE. Substrate mapping for unstable ventricular tachycardia. Heart Rhythm. 2016;13(2):569–83.

6. Higuchi T, Nakaya Y. T wave polarity related to the repolarization process of epicardial and endocardial ventricular surfaces. Am Heart J. 1984;108(2):290–5.

7. Arteyeva NV, Azarov JE. The role of transmural repolarization gradient in the inversion of cardiac electric field: model study of ECG in hypothermia. Ann Noninvasive Electrocardiol. 2017;22(1).

8. Antzelevitch C, Fish J. Electrical heterogeneity within the ventricular wall. Basic Res Cardiol. 2001;96(6):517–27.

9. Chauhan VS, Downar E, Nanthakumar K, Parker JD, Ross HJ, Chan W, et al. Increased ventricular repolarization heterogeneity in patients with ventricular arrhythmia vulnerability and cardiomyopathy: a human *in vivo* study. Am J Physiol Heart Circ Physiol. 2006;290(1):H79–86.

10. Kubala M, Pathak RK, Xie S, Casado Arroyo R, Tschabrunn CM, Hayashi T, et al. Electrocardiographic repolarization abnormalities and electroanatomic substrate in arrhythmogenic right ventricular cardiomyopathy. Circ Arrhythm Electrophysiol. 2018;11(3): e005553. https://doi.org/10.1161/CIRCEP.117.005553.

11. Ghanem RN, Burnes JE, Waldo AL, Rudy Y. Imaging dispersion of myocardial repolarization, II: noninvasive reconstruction of epicardial measures. Circulation. 2001;104(11):1306–12.

12. Opthof T, Coronel R, Wilms-Schopman FJG, Plotnikov AN, Shlapakova IN, Danilo P Jr, et al. Dispersion of repolarization in canine ventricle and the electrocardiographic T wave: Tp-e interval does not reflect transmural dispersion. Heart Rhythm. 2007;4(3): 341–8.

13. Xia Y, Liang Y, Kongstad O, Holm M, Olsson B, Yuan S. Tpeak-tend interval as an index of global dispersion of ventricular repolarization: evaluations using monophasic action potential mapping of the epi- and endocardium in swine. J Interv Card Electrophysiol. 2005;14(2):79–87.

14. Zabel M, Portnoy S, Franz MR. Electrocardiographic indexes of dispersion of ventricular repolarization: an isolated heart validation study. J Am Coll Cardiol. 1995;25(3):746–52.

15. Zabel M, et al. Comparison of ECG variables of dispersion of ventricular repolarization with direct myocardial repolarization measurements in the human heart. J Cardiovasc Electrophysiol. 1998;9(12):1279–84.

16. Taggart P, et al. Transmural repolarisation in the left ventricle in humans during normoxia and ischaemia. Cardiovasc Res. 2001;50(3):454–62.

17. Brugada J, Pappone C, Berruezo A, Vicedomini G, Manguso F, Ciconte G, et al. Brugada syndrome phenotype elimination by epicardial substrate ablation. Circ Arrhythm Electrophysiol. 2015;8(6):1373–81.

18. Garcia FC, Bazan V, Zado ES, Ren JF, Marchlinski FE. Epicardial substrate and outcome with epicardial ablation of ventricular tachycardia in arrhythmogenic right ventricular cardiomyopathy/dysplasia. Circulation. 2009;120(5):366–75.

19. Tschabrunn CM, Marchlinski FE. Ventricular tachycardia mapping and ablation in arrhythmogenic right ventricular cardiomyopathy/dysplasia: lessons learned. World J Cardiol. 2014;6(9):959–67.

20. Riley MP, Zado E, Bala R, Callans DJ, Cooper J, Dixit S, et al. Lack of uniform progression of endocardial scar in patients with arrhythmogenic right ventricular dysplasia/cardiomyopathy and ventricular tachycardia. Circ Arrhythm Electrophysiol. 2010;3(4):332–8.

21. Sosa E, et al. A new technique to perform epicardial mapping in the electrophysiology laboratory. J Cardiovasc Electrophysiol. 1996;7(6):531–6.

22. Cano O, Hutchinson M, Lin D, Garcia F, Zado E, Bala R, et al. Electroanatomic substrate and ablation outcome for suspected epicardial ventricular tachycardia in left ventricular nonischemic cardiomyopathy. J Am Coll Cardiol. 2009;54(9):799–808.

23. Campos B, Jauregui ME, Park KM, Mountantonakis SE, Gerstenfeld EP, Haqqani H, et al. New unipolar electrogram criteria to identify irreversibility of nonischemic left ventricular cardiomyopathy. J Am Coll Cardiol. 2012;60(21):2194–204.

24. Van Herendael H, et al. Idiopathic right ventricular arrhythmias not arising from the outflow tract: prevalence, electrocardiographic characteristics, and outcome of catheter ablation. Heart Rhythm. 2011;8(4):511–8.

25. Janse MJ, Coronel R, Opthof T. Counterpoint: M cells do not have a functional role in the ventricular myocardium of the intact heart. Heart Rhythm. 2011;8(6):934–7.

26. Taccardi B, Punske BB, Sachse F, Tricoche X, Colli-Franzone P, Pavarino LF, et al. Intramural activation and repolarization

sequences in canine ventricles. Experimental and simulation studies. J Electrocardiol. 2005;38(4 Suppl):131–7.

27. Janse MJ, Coronel R, Opthof T, Sosunov EA, Anyukhovsky EP, Rosen MR. Repolarization gradients in the intact heart: transmural or apico-basal? Prog Biophys Mol Biol. 2012;109(1–2):6–15.

28. Ramanathan C, Jia P, Ghanem R, Ryu K, Rudy Y. Activation and repolarization of the normal human heart under complete physiological conditions. Proc Natl Acad Sci U S A. 2006;103(16):6309–14.

29. Cowan JC, Hilton CJ, Griffiths CJ, Tansuphaswadikul S, Bourke JP, Murray A, et al. Sequence of epicardial repolarisation and configuration of the T wave. Br Heart J. 1988;60(5):424–33.

30. Castro Hevia J, Antzelevitch C, Tornés Bárzaga F, Dorantes Sánchez M, Dorticós Balea F, Zayas Molina R, et al. Tpeak-Tend and Tpeak-Tend dispersion as risk factors for ventricular tachycardia/ventricular fibrillation in patients with the Brugada syndrome. J Am Coll Cardiol. 2006;47(9):1828–34.

31. Lubinski A, et al. The terminal portion of the T wave: a new electrocardiographic marker of risk of ventricular arrhythmias. Pacing Clin Electrophysiol. 2000;23(11 Pt 2):1957–9.

32. Smetana P, Schmidt A, Zabel M, Hnatkova K, Franz M, Huber K, et al. Assessment of repolarization heterogeneity for prediction of mortality in cardiovascular disease: peak to the end of the T wave interval and nondipolar repolarization components. J Electrocardiol. 2011;44(3):301–8.

33. Yan GX, Antzelevitch C. Cellular basis for the Brugada syndrome and other mechanisms of arrhythmogenesis associated with ST-segment elevation. Circulation. 1999;100(15):1660–6.